

Research Article

Open Access



# Conductive PDA@HNT/rGO/PDMS aerogel composites with significantly enhanced durability and stretchability for wearable electronics

Hailong Hu<sup>1</sup> , Yalun Ma<sup>1</sup>, Yusuf Abdullahi Hassan<sup>1</sup>, Lei Chen<sup>2</sup>, Jing Ouyang<sup>3,4</sup>, Huaming Yang<sup>3,4</sup>, Fan Zhang<sup>3,4</sup>

<sup>1</sup>Research Institute of Aerospace Technology, Central South University, Changsha 410083, Hunan, China.

<sup>2</sup>Center of Materials Science and Optoelectronics Engineering, University of Chinese Academy of Sciences, Beijing 100049, China.

<sup>3</sup>School of Minerals Processing and Bioengineering, Central South University, Changsha 410083, Hunan, China.

<sup>4</sup>Hunan Key Laboratory of Mineral Materials and Application, Central South University, Changsha 410083, Hunan, China.

**Correspondence to:** Dr. Fan Zhang, School of Minerals Processing and Bioengineering, Central South University, No. 932, Yuelu District, Lushan South Road, Changsha 410083, Hunan, China; Hunan Key Laboratory of Mineral Materials and Application, Central South University, No. 932, Yuelu District, Lushan South Road, Changsha 410083, Hunan, China. E-mail: fan.zhang@csu.edu.cn

**How to cite this article:** Hu, H.; Ma, Y.; Hassan, Y. A.; Chen, L.; Ouyang, J.; Yang, H.; Zhang, F. Conductive PDA@HNT/rGO/PDMS aerogel composites with significantly enhanced durability and stretchability for wearable electronics. *Microstructures* 2025, 5, 2025020. <https://dx.doi.org/10.20517/microstructures.2024.121>

**Received:** 13 Nov 2024 **First Decision:** 17 Dec 2024 **Revised:** 26 Dec 2024 **Accepted:** 8 Jan 2025 **Published:** 24 Feb 2025

**Academic Editor:** Zhigang Chen **Copy Editor:** Fangling Lan **Production Editor:** Fangling Lan

## Abstract

Conductive polymer composites used to develop stretchable strain sensors have great potential for a wide range of applications, but engineering such a sensor with high sensitivity and durability remains very challenging. In this study, we propose a hydrothermal approach coupled with a freeze-drying technique to fabricate durable and stretchable strain sensors based on polydopamine-functionalized halloysite nanotube/reduced graphene oxide/polydimethylsiloxane (PDA@HNT/rGO/PDMS) aerogel composites. These sensors exhibit exceptional sensing performance, enhanced stretchability, linearity range, and stability. A comparative analysis of graphene oxide at different concentrations demonstrates that the flexible PDA@HNT/rGO/PDMS composites exhibit a significantly broader sensing range when the graphene oxide concentration is reduced to 2.5 mg/mL, in contrast to the higher concentration of 5.0 mg/mL. Specifically, the synergistic effect of both PDA and natural fiber HNTs results in aerogel composite strain sensors with a desirable gauge factor and a linearity sensing range as evidenced by the theoretical analysis, which demonstrates great potential for wearable electronics and human motion detection. The synergy between PDA and HNTs enhances the properties of aerogel composite strain sensors by



© The Author(s) 2025. **Open Access** This article is licensed under a Creative Commons Attribution 4.0 International License (<https://creativecommons.org/licenses/by/4.0/>), which permits unrestricted use, sharing, adaptation, distribution and reproduction in any medium or format, for any purpose, even commercially, as long as you give appropriate credit to the original author(s) and the source, provide a link to the Creative Commons license, and indicate if changes were made.



improving interfacial adhesion, uniformly dispersing reinforcing agents, and maintaining conductive pathways, resulting in a highly sensitive, broad-range, and durable device. The development of conductive PDA@HNT/rGO/PDMS aerogel composites for flexible strain sensors represents an important advancement in the field of wearable technology and has the potential to revolutionize the way we monitor and respond to mechanical stress in various applications.

**Keywords:** Nanocomposites, polymer-matrix composites (PMCs), finite element analysis (FEA), natural fiber HNT

## INTRODUCTION

Wearable electronic devices that are flexible have gained popularity due to their ability to respond effectively to various stimuli, including mechanical, chemical, biological, and environmental factors<sup>[1,2]</sup>. These devices can accurately monitor human health in real time, making them an essential tool for healthcare professionals. The use of innovative materials and manufacturing techniques has made these devices resistant to decomposition, ensuring their durability over time. Advanced composites and new processing technologies have also led to the development of unique devices for specific applications such as health monitoring, general movement detection, sports activity monitoring, smart textiles, and soft robotics<sup>[3,4]</sup>.

Traditional metal or semiconductor-based stress sensors have become outdated due to their limited detection and complex fabrication processes<sup>[5]</sup>. As a result, flexible and stretchable stress sensors based on polymer nanocomposites have been emerging as the most suitable alternatives<sup>[5,6]</sup>. The practical stretchable composite systems are usually designed using conductive nanofillers<sup>[7-9]</sup> in an insulating or conductive polymer matrix. In these systems, structural interface, mechanical strength, and electrical conductivity must be systematically considered to achieve optimal performance. Carbon-based nanocomposite materials, including carbon nanotubes (CNTs), carbon black (CB), carbon fibers, and graphene have been extensively studied for developing flexible strain sensors<sup>[10-16]</sup>. Other conductive fillers such as metal nanowires, nanoparticles, nanofillers, and ionic liquids are also desirable alternatives for creating flexible composite structures<sup>[17-26]</sup>. Moreover, various polymers including polyurethane (PU), polydimethylsiloxane (PDMS), thermoplastic PU (TPU), and natural rubber can be employed as flexible matrix materials to maintain nano-filler interfaces<sup>[27-32]</sup>. Conductive polymers, such as poly(3,4-ethylenedioxythiophene):poly(styrene sulfonate) (PEDOT:PSS) and polyaniline, can be incorporated into functional nanocomposite complexes to form conductive networks<sup>[33-36]</sup>. Therefore, polymer matrices support the construction of conductive networks while nanofillers confer functional sensing properties in functional nanocomposites<sup>[37]</sup>.

The working mechanism of strain-responsive functional composites can be comprehensively elucidated through the examination of their geometric interfaces, electrical conduction pathways, percolation networks, crack propagation behaviors, and tunneling effects<sup>[38-41]</sup>. The flexible strain sensor is capable of detecting changes in applied strain by altering the electrical properties of the functional composite. These sensors can be categorized as capacitive, resistance, or impedance measurement strain sensors based on the variation in their electrical properties in response to the applied strain/elongation. The performance of strain sensors is typically evaluated based on parameters such as durability, gauge factor (GF), linear range, stability, and transient response<sup>[38,42]</sup>. Conventional strain gauges require excellent mechanical robustness, high GF, low hysteresis, wide linear range, high stability, and rapid transient response. To produce flexible and stretchable strain sensors with these desired properties, nanofillers and polymer matrices are carefully selected and processed using various physical and chemical treatment techniques. However, achieving a particular set of properties may require compromising on certain performance parameters.

Current research on strain sensors has mostly focused on material detection performance, with limited success in using simple processing methods. Therefore, there is a need to develop affordable and easy methods for producing stretchable and stable strain sensors for both scientific and industrial purposes. One such advanced material developed for flexible strain sensors is the conductive PDA@HNT/rGO/PDMS aerogel composite, which is made up of polydopamine (PDA), hydroxyl nitrile triazine (HNT) nanotubes, and reduced graphene oxide (rGO). The PDA@HNT/rGO/PDMS aerogel composite is prepared by combining these three components in a specific ratio and then freeze-drying the mixture to form an aerogel. This composite has a highly porous structure, making it lightweight and flexible while maintaining its mechanical strength. Its high durability is due to the PDA coating on the HNT nanotubes providing protection against environmental factors, and the rGO layer enhancing the electrical conductivity of the composite. These properties make the PDA@HNT/rGO/PDMS aerogel composite an ideal candidate for use in flexible strain sensors, where durability and sensitivity are critical factors.

In this work, we designed stretchable and stable strain sensors with PDA@HNT/rGO in a PDMS matrix using hydrothermal and freeze-drying methods. Finite element analysis (FEA) was also performed to verify the experimental results. The conductivity, elongation, and optical transparency of the composite can be adjusted by varying the volume of PDA@HNT dispersion. HNT was used due to its high aspect ratio, large surface area, good mechanical properties, good dispersion, and low cost. The strain sensor provides a stable, fast measurement signal over a wide range of applied strains and can detect both small and large movements with high sensitivity. This transparent, stretchy strain sensor is suitable for large-scale production and has applications in health examinations, motion detection, electronic skin, and wearable electronics.

## EXPERIMENTAL DETAILS

### Materials

The PDMS silicone kit, consisting of both base and agent (Sylgard 184), was provided by Dow Corning Incorporation. Graphene oxide (GO, concentration 10 mg/mL, Jiangsu Xianfeng Nanomaterial Technology Co., Ltd.) was acquired from Sigma and used in its original state without any further treatment. Halloysite nanotubes (HNTs, diameter 10~100 nm, Shanghai Macklin Biopharmaceutical Co., Ltd.) were obtained from a commercial corporation in China and then carefully selected and purified. The other source materials used were conductive silver paste and copper wire.

### Fabrication of nanocomposite strain sensors

The process involves preparing aqueous dispersions of GO with concentrations of 2.5 and 5.0 mg/mL, then reducing GO to rGO using vitamin C. PDA is formed through *in-situ* polymerization with dihydroxyindole, indole-3-pyridone, and dopamine covalently attached to HNT. After mixing HNT, dopamine hydrochloride, and Tris in a certain ratio, the solution is centrifuged, washed, and freeze-dried to obtain PDA@HNT. Different weight ratios of HNT to GO (0:1, 1:1, 1:2, 1:4, 1:6, 1:8) are used to create a graphene hydrogel, which is then washed, freeze-dried into an aerogel, and annealed at 120 °C. A PDMS precursor is poured onto the aerogel and infiltrated under vacuum before curing at 60 °C for 24 h. Copper wires are attached using conductive silver paste to enable electrical connection.

### Experimental characterization

The microstructure of samples was characterized using a scanning electron microscope (SEM, ZEISS Sigma 300). Mechanical property tests were conducted on a tensile test machine under displacement control mode, including quasi-static tension and cyclic stretching/releasing. For the monotonic test, the strain rate was maintained at 1%/s, while for long-term stability test (such as 1,000 cycles cyclic performance), the strain rate was kept at 5%/s. The resistance change signal was recorded using Keysight.

## simulation

The study investigated various composite material models with PDMS as a matrix, using ABAQUS software to simulate and analyze the sensing performance of four designed polymer composite models. The focus was on critical parameters such as cyclic performance and GF [Supplementary Figure 1], with FEA using a static general procedure implemented to evaluate the sensing properties [Supplementary Figure 2]. The results showed that HNT fillers and PDA coating layers significantly enhance the GF and cyclic stability by optimizing the interface between the polymer matrix and fillers. The core-shell structural design of the sensing material with varying contents of PDA@HNT was used in the simulation analysis<sup>[43]</sup>.

## RESULTS AND DISCUSSION

We developed a highly stretchable and stable strain sensor by homogenizing PDA@HNT/rGO into PDMS matrices using hydrothermal and freeze-drying methods. The resulting composite exhibits excellent mechanical properties, including high flexibility and stretchability, making it suitable for use in strain sensors. The combination of PDA and HNTs enhances the overall performance of the sensor, improving dispersion and interfacial adhesion while maintaining conductive pathways, resulting in higher sensitivity and stability under stretching. This makes the sensor effective for detecting both small and large movements with high sensitivity, and its transparent nature allows for large-scale production, making it suitable for various applications such as health examinations, motion detection, electronic skin, and wearable electronics.

The cross-sectional images of the PDA@HNT/rGO/PDMS composites show varying distributions of filler materials, with different ratios of PDA@HNT to rGO, indicating the effect of surface modification on the dispersion and interfacial adhesion within the composite matrix [Supplementary Figure 3]. Transmission Electron Microscopy (TEM) images revealed the *in-situ* core-shell structured PDA@HNT nanofillers, showing their distinct morphology [Figure 1A]. High-resolution TEM imaging further elucidated the detailed architecture of the core-shell structure, where a thin layer of Polydopamine (PDA) coated the surface of HNTs [Figure 1B]. The chemical composition and bonding characteristics of the PDA@HNT nanofillers were confirmed by Fourier Transform Infrared Spectroscopy (FTIR), indicating successful surface modification [Figure 1C]. Energy Dispersive X-ray Spectroscopy (EDX or EDS) analysis was also employed to determine the elemental composition of the PDA@HNT nanofillers, verifying the presence of expected elements and the uniform distribution of PDA on the HNT surfaces [Figure 1D-I]. One of the primary functions of PDA in composite materials is its role as an adhesion promoter. The remarkable ability of PDA to form robust bonds with a diverse array of surfaces makes it an exceptional choice for enhancing the interface between dissimilar materials. This enhancement leads to improved mechanical properties, including increased tensile strength and toughness. The polymerization of dopamine (PDA) adheres to various surfaces through a combination of non-covalent interactions, such as hydrogen bonding, van der Waals forces, and  $\pi$ - $\pi$  stacking, and covalent bonding. Specifically, the amine groups within PDA can react with carboxyl or hydroxyl groups present on organic surfaces. In this work, HNTs stabilized by PDA are integrated into polymer matrices to fabricate nanocomposites with tailored properties, including enhanced mechanical characteristics and improved sensing performance.

The content of PDA plays a crucial role in determining the optical transparency and electrical properties of PDMS/HNT/PDA composites. As shown in Figure 2, increasing the content of PDA leads to progressively improved conductive networks within the composites, which enhances their sensing range performance. Conversely, decreasing the PDA content results in a reduced sensing range performance due to an increase in the thickness of the conductive layer, as illustrated in Figure 2A and B. As depicted in Figure 2C and D, the composite with a PDA content of 2.5 mg/mL at a ratio of 1:4 exhibits an optimal balance between



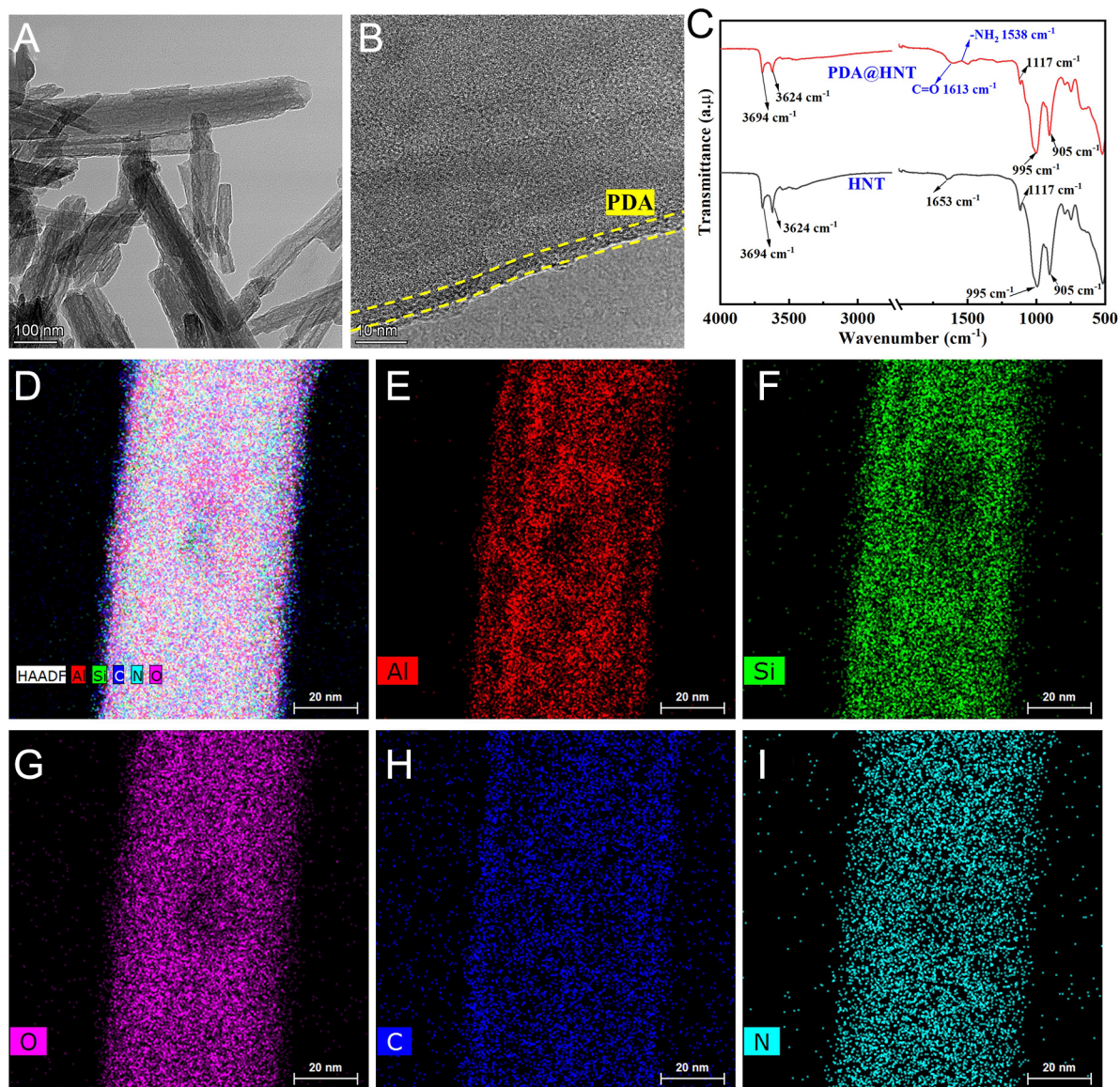


**Figure 1.** PDA@HNT nanofiller structural characterization: (A and B) TEM images of the *in-situ* core-shell structure; (C) Fourier Transform Infrared Spectrometer (FTIR) measurement; (D-I) Energy dispersive X-ray spectroscopy to verify the individual element of PDA coating at the surrounding of HNT.

sensing range and electrical resistance. In contrast, the composite with 5 mg/mL PDA displays unsatisfactory electrical properties and a relatively limited sensing range when compared to the 2.5 mg/mL PDA composite. The strain-sensing performance of the PDMS/PDA composites at different contents is investigated by observing changes in  $\Delta R/R_0$  upon stretching, as depicted in Figure 2D. It can be observed that the  $\Delta R/R_0$  values of different grades of composites increase with elongation due to fracture of the PDA-PDMS connection, resulting in fracture of the conductive path during the elongation process. Furthermore, with increasing PDA content, the strain sensing range gradually expands, while the  $\Delta R/R_0$  value tends to diminish at the same strain.

The concurrent synergistic effect of PDA and HNT in aerogel composite strain sensors is based on the enhancement of interfacial adhesion, uniform dispersion of reinforcing agents, and the maintenance of

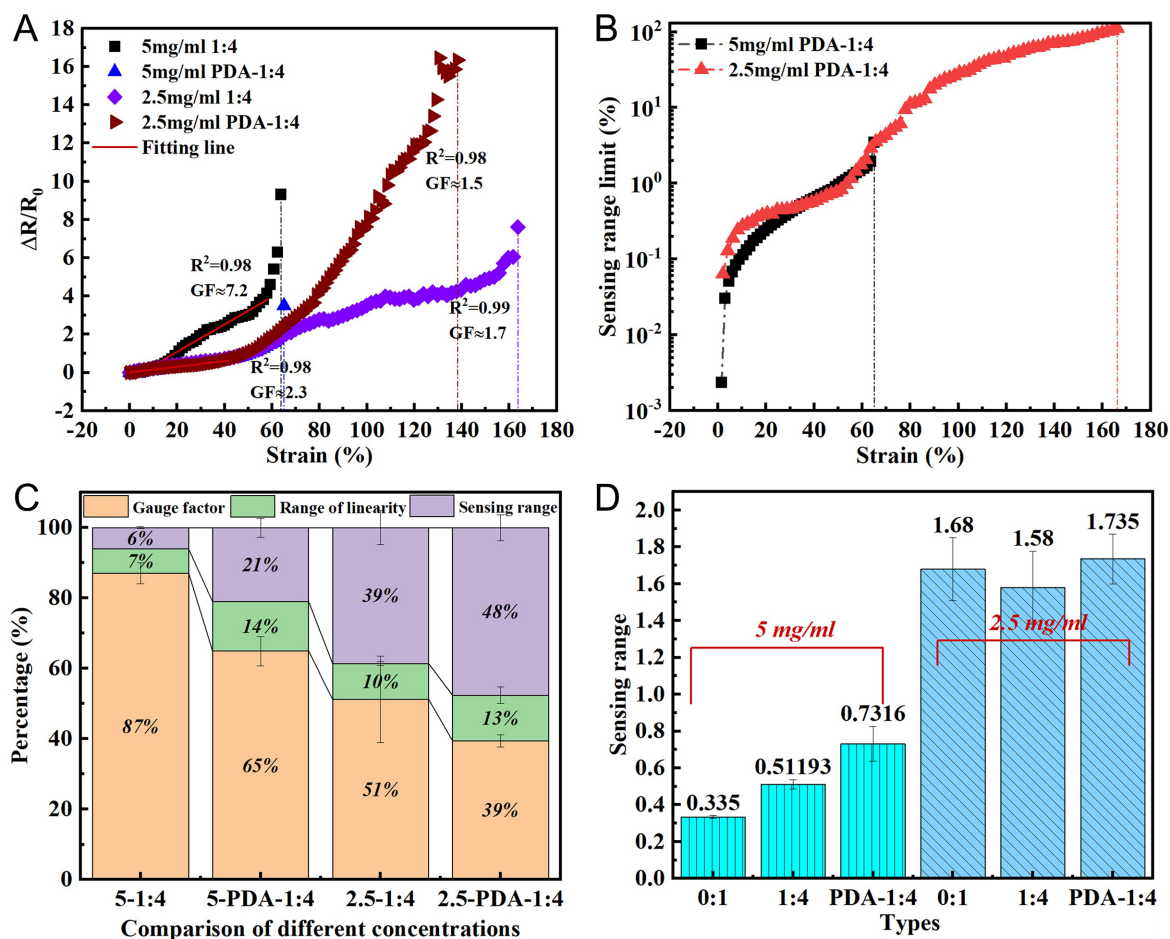


**Figure 2.** (A)  $\Delta R/R_0$  vs. applied strain to reveal gauge factor value for samples of PDA@HNT/rGO/PDMS composites; (B) relationship between the sensing range limit and strain for PDA@HNT/rGO/PDMS composites; (C) comparison of gauge factor, range of linearity and sensing range of PDA@HNT/rGO/PDMS composites; (D) Sensing performance of PDA@HNT/rGO/PDMS composites with various ratios of PDA@HNT to rGO. (Samples are analyzed at composites with concentrations of 2.5 and 5.0 mg/mL GO, respectively, where the ratio of PDA@HNT to GO is 1:4).

conductive pathways, which together improve the mechanical and electrical properties of the sensor, leading to a device with high sensitivity, wide sensing range, and good durability [Figure 3A]. To evaluate the stability and discrimination of the excellent PDA@1:4 composite strain sensors, cyclic stretching-releasing tests were conducted. As shown in Figure 3B and C, the composite strain sensors exhibit fluctuation strain detection behaviors. However, as demonstrated in Figure 3D, stable strain detection behavior is observed when the applied strain is changed. Notably, all composites exhibit a significant signal even at a strain of 0.4%. This indicates that subtle strains can be detected using PDMS/PDA composites. Furthermore, there is no apparent difference in electrical response at different strain amplitudes for PDMS/PDA composites with varying PDA levels. This phenomenon may be attributed to the fact that the applied strain is not large enough to break the connection between HNT or disrupt the conductive path. Therefore, changes in resistance of the composite material are solely caused by deformation of the conductive network.

To investigate the strain detection behavior of PDA@HNT/rGO/PDMS composites over a wide strain range, cyclic stretching-releasing tests were performed with varying strain amplitudes. In this study, 5 mg/mL PDA@HNT/rGO/PDMS composites were selected to examine their strain detection behavior. During stretching, an increase in  $\Delta R/R_0$  was observed, which may be attributed to the separation of



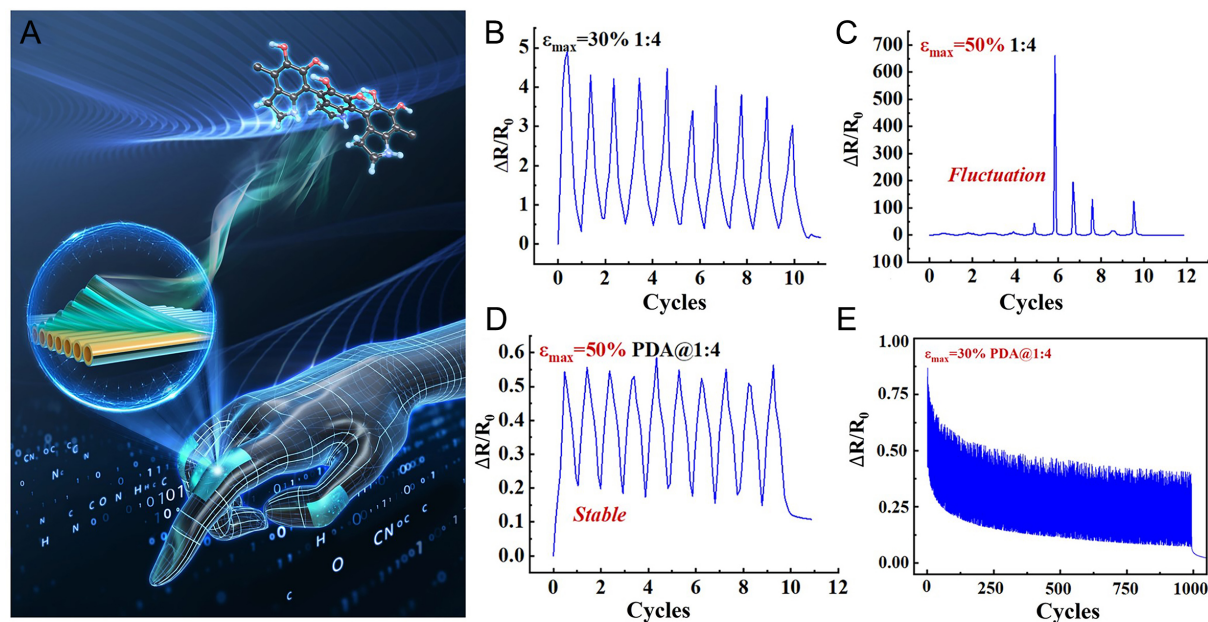


**Figure 3.** (A) Conceptual design of conductive PDA@HNT/rGO/PDMS aerogel composites with high durability for flexible strain sensors; the  $\Delta R/R_0$  performance under various cyclic strains for the PDA@HNT/rGO/PDMS composites with (B)  $\epsilon_{max} = 30\%$  1:4, (C)  $\epsilon_{max} = 50\%$  1:5, (D)  $\epsilon_{max} = 50\%$  PDA@1:4 and (E)  $\epsilon_{max} = 30\%$  PDA@1:4.

connections between rGO and the breakdown of electrically conductive pathways. Subsequently,  $\Delta R/R_0$  decreased with time during release due to the reconnection of HNT and the reestablishment of electrically conductive pathways. However, in the initial unloading process,  $\Delta R/R_0$  did not completely return to its initial value for each applied strain, as this was caused by the hysteresis effect resulting from the viscoelastic matrix and continuous damage to the conductive network<sup>[43,44]</sup>. After several stretch-release cycles, the composite exhibited stable detection signals without significant drift. The reproducibility of the strain measurement behavior of the HNT/rGO/PDMS composite under repeated tensile loadings at a maximum of 1,000 cycles is shown in Figure 3E (5 mg/mL). It was observed that the maximum value of  $\Delta R/R_0$  slightly declined in the first few cycles due to the formation of additional conductive pathways and rearrangement of conductive networks during stretching-releasing testing. Thereafter, it remained unchanged in subsequent cycles. Meanwhile, the minimum value of  $\Delta R/R_0$  also stabilized after several stretching-releasing cycles, indicating good repeatability and stability of the material. Comparing the HNT/rGO/PDMS composite with a 1:4 content [Figure 3B and C] to the one with 5 mg/mL PDA@1:4 [Figure 3D], the latter exhibited more outstanding repeatability and stability during stretching-releasing cycles due to its more perfect conductive networks.

To evaluate the strain sensing ability of HNT/rGO/PDMS composites with varying concentrations, quasi-static tensile tests were conducted. The relationship between the relative change in resistance ( $\Delta R/R_0$ ) and applied strain ( $\epsilon$ ) is shown in Figure 4A and B. It can be observed that the  $\Delta R/R_0$  values of different grades of composites increase with elongation due to fracture of the PDA-PDMS connection, resulting in fracture of the conductive path during stretching. Additionally, gradually increasing HNT content extends the strain sensing range, while the  $\Delta R/R_0$  value tends to decrease under the same strain. The experimental results in Figure 4A exhibit a good linear relationship for samples with ratios of 1:0, 1:1, 1:2, 1:4, 1:6, and 1:8, with high  $R^2$  values of 0.99, 0.92, 0.91, 0.98, 0.97, and 0.97, respectively. In Figure 4B and C, the GF of the sample (PDA@1:4) has the optimal result (GF~7.2) among the other samples mentioned earlier. Moreover, the

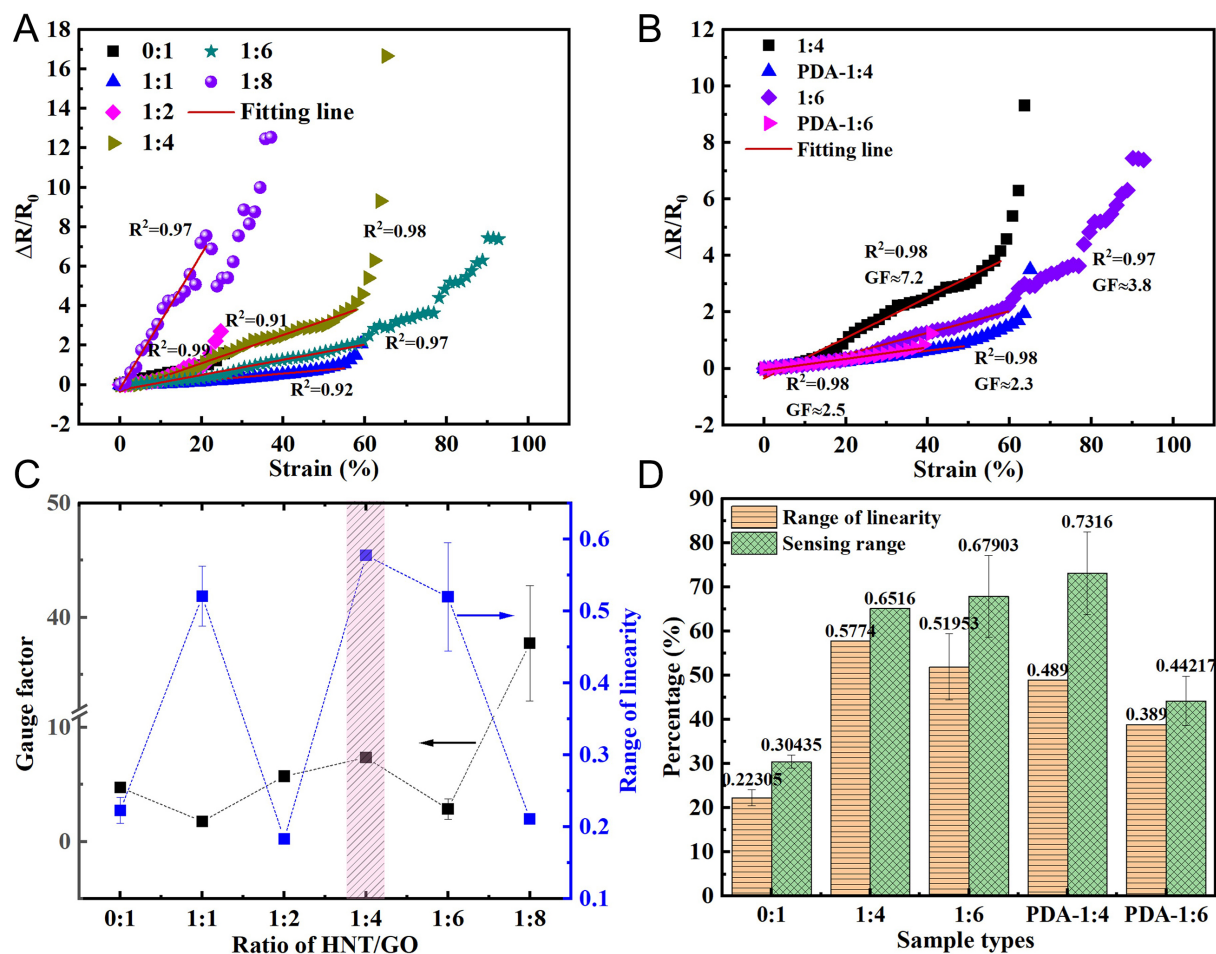


**Figure 4.** (A) The relative resistance change  $R/R_0$  of the PDA@HNT/rGO/PDMS aerogel composites vs. strain, (B)  $\Delta R/R_0$  and GF values under applied strain, (C) sensing performance of gauge factor at different HNT/GO ratios, (D) maximum percentage of sensing range and range of linearity at different ratios (PDA@HNT to GO) of samples.

maximum percentage of sensing range and range of linearity were demonstrated at different ratios (PDA@HNT to GO) of samples [Figure 4D]. Furthermore, a comparative analysis involving strain sensors utilizing alternative composite materials has been conducted, where sensing performance of varied composite strain sensors is compared with that of this work to show the advance of this achieved result, as seen in Supplementary Table 1.

To further validate/illustrate the impact of HNT fillers and PDA coating layers on enhancing cyclic performance, FEA was conducted. As depicted in Figure 5, cyclic stretching/releasing tests were performed on four distinct models (pure PDMS, 9 vol% PDA@HNT 1:4, 15 vol% PDA@HNT 1:4, and 20 vol% PDA@HNT 1:4) at a maximum elongation of 50% and a rate of 100 mm/min. The results, as shown in Figure 5A, indicate that the specimen consisting solely of polymeric material loses its sensing strength/conductive properties more rapidly under the same loading conditions compared to other specimens with core-shell structured PDA@HNT 1:4, as demonstrated in Figure 5B-D. Furthermore, the PDA@HNT composites exhibit good repeatability and stability under applied stress. Moreover, the responsiveness of the material to applied strain is a critical parameter for its application in conductive polymer composite strain sensors. The cyclic performance of neat PDMS and polymer composites with 20 vol% PDA@HNT 1:4 at

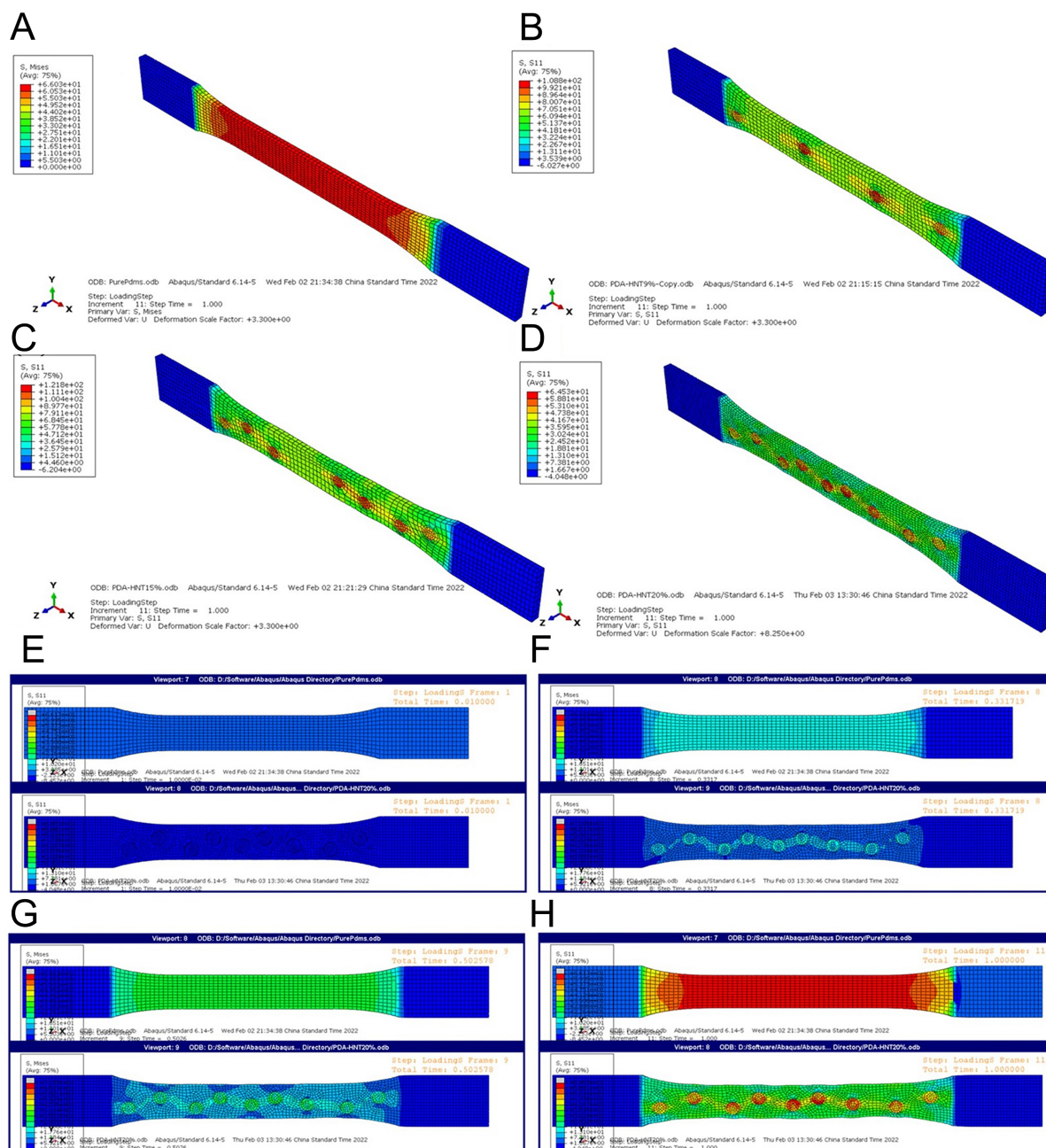


**Figure 5.** Theoretical analysis: Cyclic performance of PDA@HNT composites for (A) pure PDMS, (B) 9 vol% of PDA@HNT at 1:4, (C) 15 vol% of PDA@HNT at 1:4, (D) 20 vol% of PDA@HNT at 1:4; and cyclic performance of (E and F) pure PDMS and (G and H) 20 vol% of PDA@HNT1:4 with improved stability and stretchability under applied stress.

different iterations is presented in Figure 5E-H. It is evident that coating PDA around HNT fillers significantly enhances stability and cyclic performance, which is consistent with the experimental results obtained in this work.

Conductive PDA@HNT/rGO/PDMS aerogel composites with high durability for flexible strain sensors have significant potential in the field of wearable technology and robotics. These materials can be used to create flexible, lightweight, and durable strain sensors that can be integrated into clothing, prosthetics, and other



wearable devices<sup>[44-46]</sup>. The use of conductive PDA@HNT/rGO/PDMS aerogel composites in strain sensors allows for accurate and reliable detection of mechanical deformation, making them ideal for applications such as human motion tracking, robotic movement monitoring, and injury prevention. Additionally, their flexibility and durability make them suitable for use in harsh environments where traditional strain sensors may fail. Overall, the development of conductive PDA@HNT/rGO/PDMS aerogel composites for flexible strain sensors represents an important advancement in the field of wearable technology and has the potential to revolutionize the way we monitor and respond to mechanical stress in various applications.

An external layer of a GO sensing skeleton was integrated with a PDA-coated HNT (PDA@HNT) structural skeleton, creating a composite skeleton that combines both structural and sensing functionalities. To enhance elasticity and broaden the strain sensing range, PDMS was infused into this skeletal framework. Given that the elastic moduli of GO and HNT, constituting the sensing skeleton, exceed that of PDMS by 5-7 orders of magnitude, the interfacial sliding resistance between GO/HNT and PDMS is minimal. Consequently, during sensor deformation, predominant relative sliding occurs between GO/HNT and PDMS, with negligible deformation in the GO and HNT components themselves. This observation led to the conceptualization of the sliding GO/HNT composite skeleton as an exceptionally compliant material in our modeling approach. Based on these insights, we developed a macroscopic finite element physical model, as illustrated in [Figure 6A](#), where the details of this simulation processing are also illustrated in [Supplementary Figure 4](#). The conduction mechanism within this model is revealed, where both macroscopic sensing via the skeleton and microscopic sensing attributed to the detachment of GO flakes from the HNT surface are included. As depicted in [Figure 6B](#), computational analysis revealed the stress distribution at 30% strain for sensors incorporating varying HNT concentrations. The visual representation, through a cloud map, clearly demonstrates that sensors with elevated HNT contents exhibit more evenly distributed stress due to the augmented presence of structural skeletons, mitigating stress concentration issues. Our findings suggest that maintaining a constant quantity of the sensitive material, GO, an escalation in HNT content expands the dispersion area of the sensor's composite skeleton and augments the number of sensing pathways. This expansion translates into heightened current flow and a more conspicuous trend in current fluctuation.

To analyze the impact of the PDA coating on HNT, we compared the stress evolution during strain in PDMS matrices containing PDA-coated and uncoated HNT, as shown in [Figure 6C](#). Our results confirm that the PDA coating markedly alleviates stress concentration around HNT within PDMS, reducing the maximum observed stress by an order of magnitude. This mitigation redirects stress centralization towards the HNT core instead of the PDMS interface, thereby substantially enhancing the sensor's mechanical robustness and longevity. The investigation into the sensor's microscopic sensing mechanism revealed that changes in its electrical conductivity stem from the progressive separation and imminent separation of internal GO layers throughout the strain process. It is crucial to note that this process does not entail abrupt fractures; rather, given GO's inherent length and layered structure comprising overlapping sheets, it undergoes relative sliding alongside the PDMS matrix. This gradual reduction in overlapping area ultimately leads to complete GO sheet detachment and crack formation. Consequently, the mutual separation of graphene sheets manifests as a gradual decline in electrical conductivity. With regard to these findings, a finite element physical model, presented in [Figure 6D](#), was devised and analyzed. The model indicates that higher concentrations of HNT and GO delay the disconnection of the sensor's current, whereas lower levels of HNT or GO precipitate earlier disconnections. Furthermore, when identical voltages of 100 V were applied across the top and bottom surfaces of physical models featuring two distinct HNT contents, the upper graph in [Figure 6E](#) illustrates the cyclic current variations over three strain cycles. Additionally, the lower graph in [Figure 6E](#) calculates the GFs for the two scenarios, yielding values of 46.66

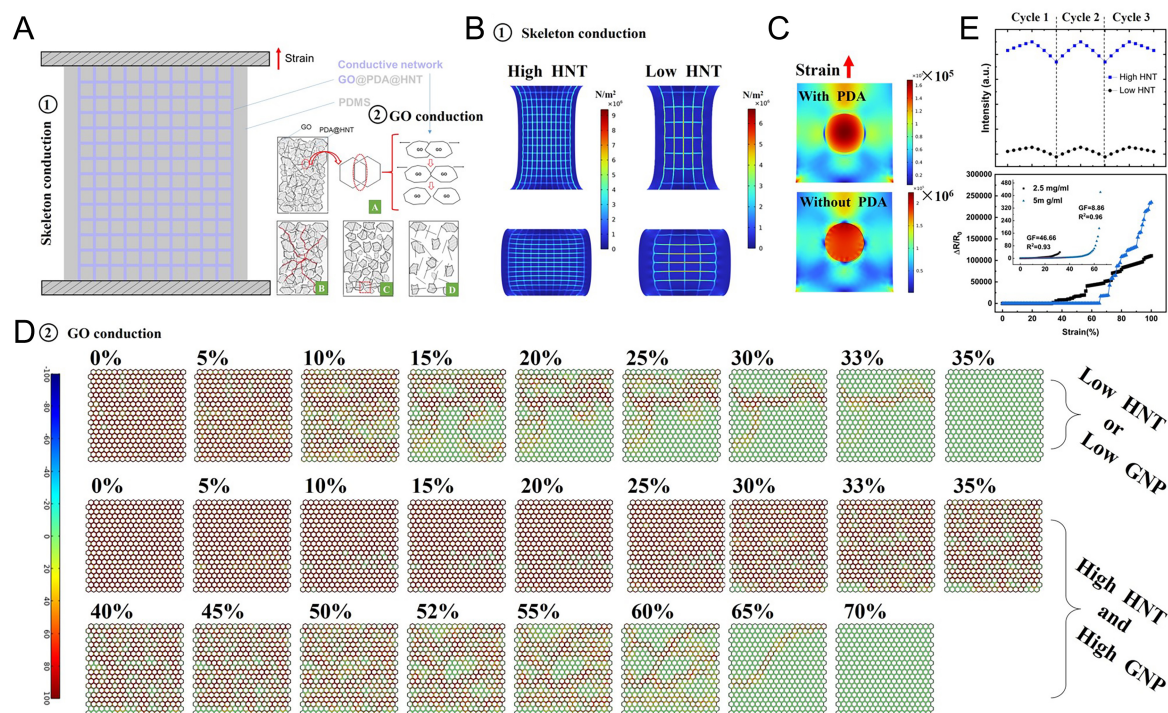


**Figure 6.** FEA analysis of sensing performance: (A) configured model, (B) the calculated stress change of the sensors with different HNT contents at 30% strain, (C) the studied stress changes of HNTs coated with PDA and uncoated with PDA in PDMS under strain, (D) finite element physical model of GO lap-joint, and (E) the gauge factors of the two models in (D) separately calculated.

and 8.86, respectively. These outcomes underscore that the dimensions of the HNT skeleton dictate the density of the GO-constructed conductive network. Specifically, as the PDA@HNT content escalates, the conductive network densifies; conversely, a decrease in HNT content yields a sparser network. This relationship implies that improving HNT content enriches the internal conductive network's complexity within the composite material. Conversely, maintaining a consistent PDA@HNT skeleton while improving GO content extends the linear strain measurement range but diminishes the sensitivity coefficient, aligning with observations reported in Figure 2.

## CONCLUSION

The superior sensing performance has been achieved in composites consisting of HNT/GO/PDMS with a HNT:GO ratio of 1:4. The incorporation of natural fiber HNT significantly improves the linearity range and sensing range/limit in HNT/GO/PDMS composites, with an increase of 158.7% and 114.1%, respectively, at the same ratio of 1:4. However, sensitivity initially increases and then decreases as the content of HNT increases. The application of a PDA coating layer around HNT further enhances the stability of the composites when subjected to cyclic testing at maximum applied strains (either  $\epsilon_{max} = 30\%$  or  $\epsilon_{max} = 50\%$ ). Furthermore, comparisons with GO at varying contents reveal that flexible GO/PDA@HNT/PDMS composites exhibit significantly enhanced sensing range at a low concentration of 2.5 mg/mL compared to that at 5.0 mg/mL. FEA is proposed to validate the role of HNT fillers and PDA coating layers in improving cyclic performance durability, showing good agreement with the achieved experimental results. Therefore, the use of conductive PDA@HNT/rGO/PDMS aerogel composites in strain sensors allows for accurate and reliable detection of mechanical deformation, making them ideal for applications such as human motion tracking, robotic movement monitoring, and injury prevention.

## DECLARATIONS

### Acknowledgment

The authors would like to appreciate the assistance from Shiyanjia Lab ([www.shiyanjia.com](http://www.shiyanjia.com)) for the help of SEM and TEM characterizations.

### Authors' contributions

Experiment, characterization, writing original draft: Hu, H.; Ma, Y.; Hassan, Y. A.; Chen, L.;  
Review & editing, supervision: Hu, H.; Ouyang, J.; Yang, H.; Zhang, F.  
Conceptualization, review, supervision: Zhang, F.

### Availability of data and materials

The data supporting the findings of this study are available within this Article and its [Supplementary Material](#). Further data are available from the corresponding authors upon request.

### Financial support and sponsorship

This work was supported by the National Natural Science Foundation of China (52204299), Natural Science Foundation of Hunan Province (2022JJ40623 and 2022JJ30722) and Start-Up Funds for Outstanding Talents in Central South University through projects of 202045007 and 202044017.

### Conflicts of interest

All authors declared that there are no conflicts of interest.

### Ethical approval and consent to participate

Not applicable.

### Consent for publication

Not applicable.

### Copyright

© The Author(s) 2025.

## REFERENCES

1. Kumar K, Chen PY, Ren H. A review of printable flexible and stretchable tactile sensors. *Research* **2019**, 2019, 3018568. [DOI](#) [PubMed](#) [PMC](#)
2. Mohammed, A. M.; Maddipatla, D.; Narakathu, B. B.; et al. Printed strain sensor based on silver nanowire/silver flake composite on flexible and stretchable TPU substrate. *Sensors. Actuators. A. Phys.* **2018**, 274, 109-15. [DOI](#)
3. Hassan Y, Hu H. Current status of polymer nanocomposite dielectrics for high-temperature applications. *Compos. Part. A. Appl. Sci. Manuf.* **2020**, 138, 106064. [DOI](#)
4. Hu, H.; Zhang, F.; Luo, S.; Chang, W.; Yue, J.; Wang, C. H. Recent advances in rational design of polymer nanocomposite dielectrics for energy storage. *Nano. Energy.* **2020**, 74, 104844. [DOI](#)
5. Yan, T.; Wang, Z.; Pan, Z. J. Flexible strain sensors fabricated using carbon-based nanomaterials: a review. *Curr. Opin. Solid. State. Mater. Sci.* **2018**, 22, 213-28. [DOI](#)
6. Fan, X.; Liu, Y.; Zhang, G.; et al. Optimization of mechanical property and sensing performance in CNF/fly ash-based geopolymer composites. *J. Cent. South. Univ.* **2024**, 55, 907-17. [DOI](#)
7. Aziz, S.; Jung, K. C.; Chang, S. H. Stretchable strain sensor based on a nanocomposite of zinc stannate nanocubes and silver nanowires. *Compos. Struct.* **2019**, 224, 111005. [DOI](#)
8. Fang, W.; Jang, H. W.; Leung, S. N. Evaluation and modelling of electrically conductive polymer nanocomposites with carbon nanotube networks. *Compos. Part. B. Eng.* **2015**, 83, 184-93. [DOI](#)
9. Fu, R.; Zhao, X.; Zhang, X.; Su, Z. Design strategies and applications of wearable piezoresistive strain sensors with dimensionality-based conductive network structures. *Chem. Eng. J.* **2025**, 454, 140467. [DOI](#)
10. Njuguna, M. K.; Yan, C.; Hu, N.; Bell, J. M.; Yarlagadda, P. K. D. V. Sandwiched carbon nanotube film as strain sensor. *Compos. Part. B. Eng.* **2012**, 43, 2711-7. [DOI](#)

11. Zhang, W.; Liu, Q.; Chen, P. Flexible strain sensor based on carbon black/silver nanoparticles composite for human motion detection. *Materials* **2018**, *11*, 1836. DOI PubMed PMC
12. Yang, Y.; Wang, H.; Hou, Y.; et al. MWCNTs/PDMS composite enabled printed flexible omnidirectional strain sensors for wearable electronics. *Compos. Sci. Technol.* **2022**, *226*, 109518. DOI
13. Zhang, F.; Wu, S.; Peng, S.; Sha, Z.; Wang, C. H. Synergism of binary carbon nanofibres and graphene nanoplates in improving sensitivity and stability of stretchable strain sensors. *Compos. Sci. Technol.* **2019**, *172*, 7-16. DOI
14. Zhang, F.; Hu, H.; Islam, M.; et al. Multi-modal strain and temperature sensor by hybridizing reduced graphene oxide and PEDOT:PSS. *Compos. Sci. Technol.* **2020**, *187*, 107959. DOI
15. Zhang, F.; Wu, S.; Peng, S.; Wang, C. H. The effect of dual-scale carbon fibre network on sensitivity and stretchability of wearable sensors. *Compos. Sci. Technol.* **2018**, *165*, 131-9. DOI
16. Hu, H.; Ma, Y.; Yue, J.; Zhang, F. Porous GNP/PDMS composites with significantly reduced percolation threshold of conductive filler for stretchable strain sensors. *Compos. Commun.* **2022**, *29*, 101033. DOI
17. Fan, X.; Hu, H.; Liao, B.; Zhang, Y.; Zhang, F. Optimization of microstructure design for enhanced sensing performance in flexible piezoresistive sensors. *J. Adv. Ceram.* **2024**, *13*, 711-28. DOI
18. Hassan, M.; Liu, S.; Liang, Z.; et al. Revisiting traditional and modern trends in versatile 2D nanomaterials: synthetic strategies, structural stability, and gas-sensing fundamentals. *J. Adv. Ceram.* **2023**, *12*, 2149-246. DOI
19. Soe, H. M.; Abd, M. A.; Matsuda, A.; Jaafar, M. Performance of a silver nanoparticles-based polydimethylsiloxane composite strain sensor produced using different fabrication methods. *Sensors. Actuators. A. Phys.* **2021**, *329*, 112793. DOI
20. Chen, X.; Zhao, X.; Huang, X.; et al. Flexible multilevel nonvolatile biocompatible memristor with high durability. *J. Nanobiotechnol.* **2023**, *21*, 375. DOI PubMed PMC
21. Wang, C.; Xu, Q.; Hu, J.; et al. Graphene/SiC-coated textiles with excellent electromagnetic interference shielding, Joule heating, high-temperature resistance, and pressure-sensing performances. *J. Adv. Ceram.* **2023**, *12*, 778-91. DOI
22. Hu, H.; Zhang, F. Rational design of self-powered sensors with polymer nanocomposites for human-machine interaction. *Chin. J. Aeronaut.* **2022**, *35*, 155-77. DOI
23. Soomro, A. M.; Khalid, M. A. U.; Shah, I.; Kim, S. W.; Kim, Y. S.; Choi, K. H. Highly stable soft strain sensor based on Gly-KCl filled sinusoidal fluidic channel for wearable and water-proof robotic applications. *Smart. Mater. Struct.* **2020**, *29*, 025011. DOI
24. Bu, Y.; Shen, T.; Yang, W.; et al. Ultrasensitive strain sensor based on superhydrophobic microcracked conductive Ti<sub>3</sub>C<sub>2</sub>T<sub>x</sub> MXene/paper for human-motion monitoring and E-skin. *Sci. Bull.* **2021**, *66*, 1849-57. DOI
25. Dong, H.; Sun, J.; Liu, X.; Jiang, X.; Lu, S. Highly sensitive and stretchable MXene/CNTs/TPU composite strain sensor with bilayer conductive structure for human motion detection. *ACS. Appl. Mater. Interfaces.* **2022**, *14*, 15504-16. DOI
26. Chen, T.; Xie, Y.; Wang, Z.; et al. Recent advances of flexible strain sensors based on conductive fillers and thermoplastic polyurethane matrixes. *ACS. Appl. Polym. Mater.* **2021**, *3*, 5317-38. DOI
27. Li, M.; Li, H.; Zhong, W.; Zhao, Q.; Wang, D. Stretchable conductive polypyrrole/polyurethane (PPy/PU) strain sensor with netlike microcracks for human breath detection. *ACS. Appl. Mater. Interfaces.* **2014**, *6*, 1313-9. DOI
28. Chen, J.; Zhu, Y.; Jiang, W. A stretchable and transparent strain sensor based on sandwich-like PDMS/CNTs/PDMS composite containing an ultrathin conductive CNT layer. *Compos. Sci. Technol.* **2020**, *186*, 107938. DOI
29. Qin, Y.; Peng, Q.; Ding, Y.; et al. Lightweight, superelastic, and mechanically flexible graphene/polyimide nanocomposite foam for strain sensor application. *ACS. Nano.* **2015**, *9*, 8933-41. DOI
30. Boland, C. S.; Khan, U.; Backes, C.; et al. Sensitive, high-strain, high-rate bodily motion sensors based on graphene-rubber composites. *ACS. Nano.* **2014**, *8*, 8819-30. DOI
31. Xu, R.; Lu, Y.; Jiang, C.; et al. Facile fabrication of three-dimensional graphene foam/poly(dimethylsiloxane) composites and their potential application as strain sensor. *ACS. Appl. Mater. Interfaces.* **2014**, *6*, 13455-60. DOI
32. Tian, H.; Shu, Y.; Cui, Y. L.; et al. Scalable fabrication of high-performance and flexible graphene strain sensors. *Nanoscale* **2014**, *6*, 699-705. DOI
33. Kang, S.; Pradana, R. V.; Baek, J.; Lee, S. Y.; Park, S. A flexible patch-type strain sensor based on polyaniline for continuous monitoring of pulse waves. *IEEE. Access.* **2020**, *8*, 152105-15. DOI
34. Qian, Q.; Wang, Y.; Zhang, M.; et al. Ultrasensitive paper-based polyaniline/graphene composite strain sensor for sign language expression. *Compos. Sci. Technol.* **2019**, *181*, 107660. DOI
35. Shao, G.; Jiang, J.; Jiang, M.; et al. Polymer-derived SiBCN ceramic pressure sensor with excellent sensing performance. *J. Adv. Ceram.* **2020**, *9*, 374-9. DOI
36. Xue, S.; Tang, Z.; Zhu, W.; Li, Y.; Huang, P.; Fu, S. Stretchable and ultrasensitive strain sensor from carbon nanotube-based composite with significantly enhanced electrical and sensing properties by tailoring segregated conductive networks. *Compos. Commun.* **2022**, *29*, 100987. DOI
37. Khalid, M. A. U.; Chang, S. H. Flexible strain sensors for wearable applications fabricated using novel functional nanocomposites: a review. *Compos. Struct.* **2022**, *284*, 115214. DOI
38. Souril, H.; Banerjee, H.; Jusufi, A.; et al. Wearable and stretchable strain sensors: materials, sensing mechanisms, and applications. *Adv. Intell. Syst.* **2020**, *2*, 2000039. DOI
39. Liu, H.; Li, Q.; Zhang, S.; et al. Electrically conductive polymer composites for smart flexible strain sensors: a critical review. *J. Mater. Chem. C.* **2018**, *6*, 12121-41. DOI

40. Hu, H. Recent advances of polymeric phase change composites for flexible electronics and thermal energy storage system. *Compos. Part. B. Eng.* **2020**, *195*, 108094. [DOI](#)
41. Hu, N.; Karube, Y.; Yan, C.; Masuda, Z.; Fukunaga, H. Tunneling effect in a polymer/carbon nanotube nanocomposite strain sensor. *Acta. Mater.* **2008**, *56*, 2929-36. [DOI](#)
42. Zhang, F.; Hu, H.; Hu, S.; Yue, J. Significant strain-rate dependence of sensing behavior in TiO<sub>2</sub>@carbon fibre/PDMS composites for flexible strain sensors. *J. Adv. Ceram.* **2021**, *10*, 1350-9. [DOI](#)
43. Abdullahi, H. Y.; Chen, L.; Geng, X.; et al. Electrocaloric effect of structural configured ferroelectric polymer nanocomposites for solid-state refrigeration. *ACS. Appl. Mater. Interfaces.* **2021**, *13*, 46681-93. [DOI](#)
44. Zhou, Q.; Wang, Y.; Zhu, T.; Lian, M.; Nguyen, D. H.; Zhang, C. Highly stretchable, self-healable and wide temperature-tolerant deep eutectic solvent-based composite ionogels for skin-inspired strain sensors. *Compos. Commun.* **2023**, *41*, 101658. [DOI](#)
45. Ma, Z.; Zhang, Y.; Jiang, R.; et al. Highly stretchable and room-temperature self-healing sheath-core structured composite fibers for ultrasensitive strain sensing and visual thermal management. *Compos. Sci. Technol.* **2024**, *248*, 110460. [DOI](#)
46. Wang, X.; Wang, G.; Liu, W.; et al. Developing a carbon composite hydrogel with a highly conductive network to improve strain sensing performance. *Carbon* **2024**, *216*, 118500. [DOI](#)